Quantum mechanical and semi-classical treatment of quantum excitations due to the passage of a particle

2003 J. Phys. A: Math. Gen. 36 5625

(http://iopscience.iop.org/0305-4470/36/20/318)

INSTITUTE OF PHYSICS PUBLISHING JOURNAL OF PHYSICS A: MATHEMATICAL AND GENERAL

J. Phys. A: Math. Gen. **36** (2003) 5625–5643 PII: S0305-4470(03)60238-6

Quantum mechanical and semi-classical treatment of quantum excitations due to the passage of a particle

W van Dijk[1,2], K A Kiers[3], Y Nogami[2], A Platt[3] and K Spyksma[1,4]

[1] Redeemer University College, Ancaster, Ontario, Canada L9K 1J4
[2] Department of Physics and Astronomy, McMaster University, Hamilton, Ontario, Canada L8S 4M1
[3] Department of Physics, Taylor University, Upland, IN 46989-1001, USA

E-mail: vandijk@physics.mcmaster.ca

Received 28 February 2003
Published 7 May 2003
Online at stacks.iop.org/JPhysA/36/5625

Abstract

We examine the validity of the approximation in which an α particle interacting with an atom is treated classically. In order to analyse such interactions, we perform a model simulation in which the α particle is considered as a particle in one dimension, and the atom as a quantum two-level system. The particle impinges on and excites the two-level system. We treat the particle in two ways: as a quantum mechanical wave packet, and as a classical particle. The classical particle may be a point or may have an extended structure. In each case we calculate the excitation probability $P_{21}(t)$ as a function of time t. We focus on the situation in which the kinetic energy of the incident particle well exceeds the excitation energy of the two-level system. Although the finite-time behaviour of $P_{21}(t)$ varies, $P_{21}(\infty)$ is remarkably insensitive to the size and shape of the incident wave packet in the quantum mechanical treatment. In the classical treatment, in contrast, we find that $P_{21}(\infty)$ is sensitive to the size of the particle. The classical point particle, however, yields nearly the same values of $P_{21}(\infty)$ as the quantum wave packet. Implications of the results on the interaction between an α particle and an atom are discussed.

PACS numbers: 03.65.Nk, 03.65.sq, 23.60.+e

1. Introduction

In some circumstances subatomic particles are treated classically even while they are inducing quantum mechanical transitions in systems with which they interact. For example, the cloud chamber tracks formed by charged particles emitted from nuclei of atoms are well defined and

[4] Present address: Department of Atmospheric and Oceanic Sciences, McGill University, Montreal, Quebec, Canada H3A 2K6.

seem to indicate classical trajectories for the emitted particles. Another interesting example is the ionization of an atom due to α (or β) particle emission from the nucleus of the atom. The traditional calculation for the ionization probability assumes that the α particle is a point charge that is suddenly emitted from the nucleus at a certain time. Once it is outside the nucleus, the α particle follows a classical trajectory and then interacts quantum mechanically with the atomic electrons [1, 2].

In the classical treatment, the α particle passes by the atomic electrons with great speed so that the electric field at the electrons changes rapidly. Furthermore, the nuclear charge changes suddenly when the α particle is emitted. Quantum mechanically, however, the Schrödinger wave associated with the α particle leaks out from the nucleus, usually very slowly. The electric field due to the α particle is related to the α particle's probability density, which varies slowly in time, especially if the half-life of the parent nucleus is large. In this case one anticipates an almost adiabatic process with little or no atomic transition taking place, whereas in the classical case one could employ the sudden approximation since the electric field changes rapidly. On this ground, one would expect different results in the classical and quantum mechanical treatment of the α particle. It is intriguing that the treatment involving classical trajectories gives results that are in reasonable agreement with experiment [1–4].

Regarding the cloud chamber tracks, the problem of reconciling the classical behaviour of the α particle with quantum theory was attempted early in the development of quantum mechanics by Mott [5]. For the atomic ionization caused by the nuclear α decay, justification of the classical treatment of the α particle was given by Révai and Nogami [6]. These processes are intrinsically time dependent. However, Mott and Révai–Nogami treated the problems as those of stationary or quasi-stationary states. The atomic ionization caused by the nuclear α decay was re-examined recently and the time-dependent aspect of the problem was addressed within the context of a schematic model that simulated the ionization process [7–9]. It was found that a fully quantum mechanical, time-dependent calculation gives results for the ionization probability that are orders of magnitude smaller than those of the calculation with a classical α particle. These results are inconsistent with those of Révai and Nogami [6].

A similar situation arises with the recent measurements and discussion of the bremsstrahlung emission in α decay [10–15]. Here the issues are whether the α particle can be considered as a classical particle accelerating in the Coulomb field of the daughter nucleus with the consequent electromagnetic radiation, whether the radiation during the tunnelling part of the process ought to be included, and whether a full quantum calculation yields results that agree with experiment [9].

While it is relatively common practice to use a mixed classical-quantum approach when considering the interactions of an α particle with its environment, it is not at all clear that such an approach should lead to sensible results. The purpose of this paper is to demonstrate that there are situations in which the classical treatment of the α particle gives nearly the same results asymptotically (i.e., at large times) as a fully quantum mechanical treatment. In order to compare the two approaches, we construct a simple model in which a travelling particle interacts with an excitable quantum system. In the calculations below, the travelling particle is treated both quantum mechanically and classically. In the former case, the time-dependent Schrödinger equation governs the time evolution of the quantum mechanical wave packet representing the incident particle. In the latter case, the incident particle is treated classically and is assumed to travel at a specified, constant speed. The object of the exercise is to determine the conditions for which the two approaches give similar results.

The model used is one dimensional and it involves a two-level quantum system. The quantum or classical particle simulates the α particle and the two-level system simulates an atom that can be energetically excited by the passage of the particle. We find that the quantum

mechanical and the classical point-particle approaches lead to similar results for the transition probability for the two-level system at large times. This approximate agreement holds when the kinetic energy of the incident particle is significantly larger than the excitation energy of the two-level system, which condition obtains with the α–atom interaction. As the kinetic energy becomes smaller, the agreement deteriorates.

In section 2 we set up the fully quantum mechanical version of the model in which the incident particle is represented by a wave packet. We study the effect of the width and the shape of the wave packet on the excitation of the two-level system. In section 3 we approximate the system in the following ways. First, in section 3.1 we assume that the incident particle is not a wave packet, but rather a classically moving point particle. Second, in section 3.2 we assume that the incident particle is again a classically moving particle, but that it has an extended structure. In section 4 the results are summarized and discussed. Implications on the interaction between the α particle and the atom are explored.

2. Excitation of a two-level system by the passage of a wave packet

In this section we consider the quantum mechanical version of the model, taking the incident particle to be represented by a wave packet. We employ two separate functional forms for the initial wave packet, using a Gaussian envelope to simulate a free incident particle and a truncated exponential envelope to simulate a particle emitted during a nuclear decay. In each case, the incident wave packet interacts with a quantum two-level system.

The Hamiltonian H_0 of the two-level system has eigenstates $|i\rangle$ and corresponding energy eigenvalues ϵ_i,

$$H_0|i\rangle = \epsilon_i|i\rangle \qquad \text{for} \quad i = 1, 2 \tag{1}$$

where $\epsilon_2 > \epsilon_1$, i.e., $|1\rangle$ is the ground state and $|2\rangle$ is the excited state. These two states are orthonormal. This Hamiltonian is in the spirit of a general two-state composite detector discussed in [16–18].

The incident particle has mass m and interacts with the quantum two-level system, which is initially in its ground state. The system can be excited by the incident particle due to the interaction

$$H_{\text{int}} = V(x)(|1\rangle\langle 2| + |2\rangle\langle 1|) \tag{2}$$

where x is the position of the particle. For simplicity, we assume that diagonal terms, $|1\rangle\langle 1|$ and $|2\rangle\langle 2|$, are absent from H_{int}. The Hamiltonian of the combined particle and two-level system is

$$\begin{aligned} H &= H_{\text{kin}} + H_0 + H_{\text{int}} \\ &= \sum_{i=1}^{2}\left(-\frac{\hbar^2}{2m}\frac{\partial^2}{\partial x^2} + \epsilon_i\right)|i\rangle\langle i| + \sum_{\substack{i,j=1 \\ i\neq j}}^{2} V(x)|i\rangle\langle j| \end{aligned} \tag{3}$$

where H_{kin} refers to the kinetic energy part of the Hamiltonian. For $V(x)$ we choose a Gaussian function

$$V(x) = \lambda(\beta/\sqrt{\pi})\,\mathrm{e}^{-\beta^2x^2}. \tag{4}$$

Note that $\int_{-\infty}^{\infty} V(x)\,\mathrm{d}x = \lambda$. The two-level system is fixed at the origin and the interaction region is confined around the origin. The Hamiltonian H is invariant under the simultaneous transformations of $V(x) \to -V(x)$ and $|2\rangle \to -|2\rangle$. The physics of the system is independent of the sign of $V(x)$.

In the following we use atomic units throughout so that $\hbar = 1$. The units of length, mass and energy are the Bohr radius, the electron mass and 1 Hartree = 27.2 eV, respectively. The speed of light is $c = 137.0$. For the energy levels, we assume $\epsilon_1 = 0$ and $\epsilon_2 = 1$. For the mass m, we somewhat arbitrarily assume $m = 100$. This value is to simulate the mass of the α particle, which is actually much larger. For the speed of the incident particle we take $v = 1$ in most of the cases that we examine. Then the kinetic energy of the incident particle is $\frac{1}{2}mv^2 = 50$, which is much larger than the excitation energy, $\epsilon_2 - \epsilon_1 = 1$, of the two-level system. The range of the interaction we fix by taking $\beta = 1$. For the strength parameter λ of the interaction, we take three values, 0.1, 2.0 and 10.0. Among these values, $\lambda = 2.0$ is probably the most appropriate choice as a simulation for the α–atom interaction. In this connection recall that the potential $-2\delta(x)$ can be taken as a one-dimensional simulation of the Coulomb potential between an α particle and an electron [19–21].

We solve the time-dependent Schrödinger equation

$$\left(\mathrm{i}\frac{\partial}{\partial t} - H\right)\Psi(x,t) = 0 \tag{5}$$

with

$$\Psi(x,t) = \psi_1(x,t)|1\rangle + \psi_2(x,t)|2\rangle \tag{6}$$

and taking the initial condition at $t = t_0$ to be

$$\psi_1(x,t_0) = \phi(x - x_0)\,\mathrm{e}^{\mathrm{i}k(x-x_0)} \qquad \psi_2(x,t_0) = 0. \tag{7}$$

The function $\phi(x - x_0)\,\mathrm{e}^{\mathrm{i}k(x-x_0)}$ specifies the initial shape of the wave packet that is incident on the interaction region. The position x_0 (<0) denotes the centre of the wave packet in the case of the Gaussian envelope and the 'leading edge' of the wave packet in the case of the truncated exponential envelope. The factor $\mathrm{e}^{\mathrm{i}kx}$ causes the wave packet to move with speed $v = k/m > 0$ to the right towards the origin. The probability of transition to the excited state of the two-level system at time t is

$$P_{21}(t) = \int_{-\infty}^{\infty} |\psi_2(x,t)|^2\,\mathrm{d}x. \tag{8}$$

In spite of the apparent simplicity of the model, the numerical solution of equation (5) proved highly nontrivial. The elementary approach of the basic Crank–Nicolson method of solving the partial differential equation was inadequate. The improved higher order Crank–Nicolson method suggested in [22] is promising, but we used a numerical procedure based on the Chebyshev expansion of the time evolution operator combined with the fast Fourier method of the spatial dependence for calculating the Hamiltonian operation [23, 24]. The advantage of the latter method is that one does not need to reach the final time by making small time increments. The improved Crank–Nicolson method on the other hand ensures the preservation of unitarity throughout.

As noted above, we consider two different functional forms for the envelope of the initial wave packet. The first represents a free travelling wave packet and is denoted by $\phi_a(x)$, while the second corresponds to the shape associated with a particle emitted by a decaying system and is denoted by $\phi_b(x)$.

2.1. Free travelling wave packet

The wave packet of a free travelling particle is usually taken to have an envelope of the Gaussian shape, so that

$$\phi_a(x - x_0) = (2\pi\,\Delta^2)^{-1/4}\,\mathrm{e}^{-[(x-x_0)/(2\Delta)]^2} \tag{9}$$

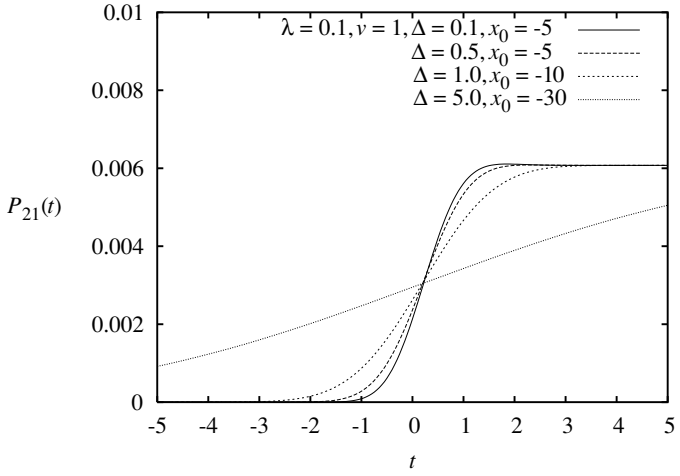

Figure 1. Transition probability from state 1 to state 2 for a Gaussian wave packet with speed $v = 1$ and different widths. The parameters are $m = 100$, $\epsilon_1 = 0$, $\epsilon_2 = 1$, $\lambda = 0.1$ and $\beta = 1$.

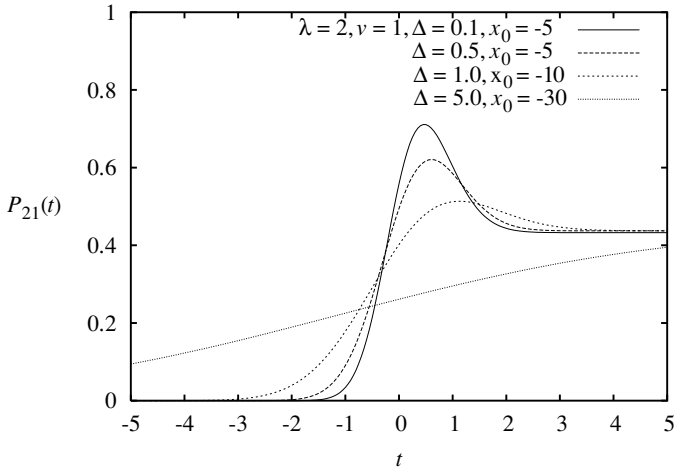

Figure 2. Transition probability from state 1 to state 2 with parameters as in figure 1 except that $\lambda = 2$.

where $\Delta > 0$ is the width of the wave packet. Note that $\int_{-\infty}^{\infty} \phi_a^2(x)\,\mathrm{d}x = 1$ and $\int_{-\infty}^{\infty} \phi_a^2(x)x^2\,\mathrm{d}x = \Delta^2$. We choose $x_0 \ll -\Delta$ and $x_0 \ll -1/\beta$ so that the initial wave packet is well outside the interaction region.

Figures 1, 2 and 3 show $P_{21}(t)$ versus t for a wave packet incident with speed $v = 1$, but for a number of cases with different widths Δ. We have chosen the time reference such that the free particle would have passed the origin at $t = 0$, i.e., the initial time t_0 is negative and $x_0 = vt_0$. As the width Δ increases the curve is smeared out in time, but as $t \to \infty$ the transition probability $P_{21}(t)$ approaches nearly the same value regardless of the width of the wave packet. Table 1 shows $P_{21}(\infty)$ for the various cases. When $\Delta = \infty$, the wave packet actually becomes a plane wave. (See appendix A.) The values obtained for $P_{21}(\infty)$ for Gaussian wave packets are remarkably insensitive to Δ and are also close to the values

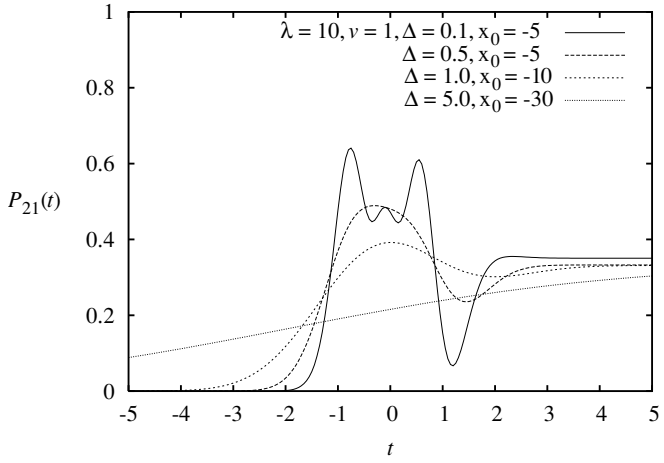

Figure 3. Transition probability from state 1 to state 2 with parameters as in figure 1 except that $\lambda = 10$.

Table 1. Numerical results for $P_{21}(\infty)$ for Gaussian wave packets with different values of λ and Δ when $m = 100$, $\epsilon_1 = 0$, $\epsilon_2 = 1$, $v = 1$ and $\beta = 1$. The last row gives the results for the classical point-particle approximation described in section 3.1.

	$\lambda = 0.1$	$\lambda = 2.0$	$\lambda = 10.0$
$\Delta = 0.1$	0.006 073	0.432 54	0.350 49
$\Delta = 0.5$	0.006 074	0.437 16	0.332 68
$\Delta = 1.0$	0.006 074	0.437 31	0.331 38
$\Delta = 5.0$	0.006 074	0.437 36	0.330 95
$\Delta = \infty$	0.006 074	0.437 36	0.330 93
Classical point	0.006 044	0.445 26	0.285 06

obtained for the passage of a classical point particle (see section 3.1), as the last line of table 1 shows.

The profiles of $P_{21}(t)$ shown in figures 1, 2 and 3 depend on the initial starting position x_0 of the wave packet. If the packet is started further out it will have broadened by the time it gets to the interaction region and displays behaviour more like that of a wave packet with larger Δ. What is surprising is that wave packets of the same width starting at different initial locations give exactly the same values for $P_{21}(\infty)$, even though the $P_{21}(t)$ profiles are quite different. We show in figure 4 the transition probability $P_{21}(t)$ for four different starting positions of the same wave packet. Even though the graphs are different the asymptotic values are the same within numerical uncertainty for all four cases, i.e., $P_{21}(\infty) = 0.350\,491\,9001$.

For the parameters used in the calculation, the reflection of the wave packet from the interaction region is negligible both for $\psi_1(x, t)$ and $\psi_2(x, t)$. The propagation of the wave packets $\psi_1(x, t)$ and $\psi_2(x, t)$ is compared to that of a free wave packet in figure 5. If we reduce the range $1/\beta$ of the interaction, the reflection becomes more appreciable. See appendix A for a discussion of the limit of $\beta \to \infty$ and $V(x) \to \lambda\delta(x)$.

2.2. Wave packet from a decaying system

Of particular interest in the present work is the case in which an α particle is ejected in the radioactive decay of a nucleus and interacts with an excitable system, e.g., an atom. The α

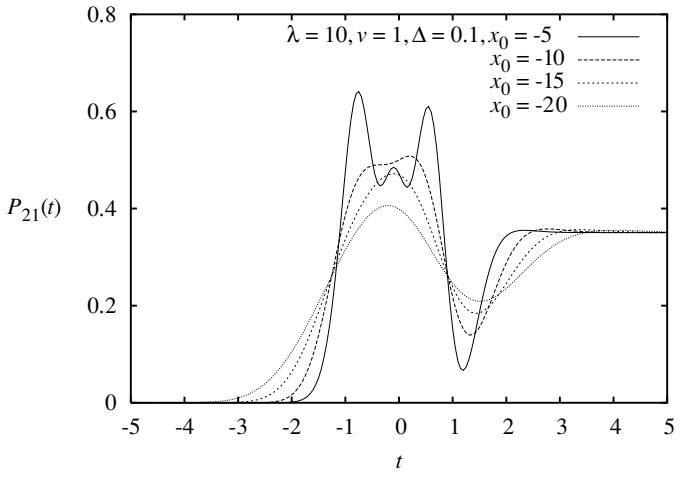

Figure 4. Transition probability as a function of time from state 1 to state 2 with a single set of parameters but different starting positions of the wave packet.

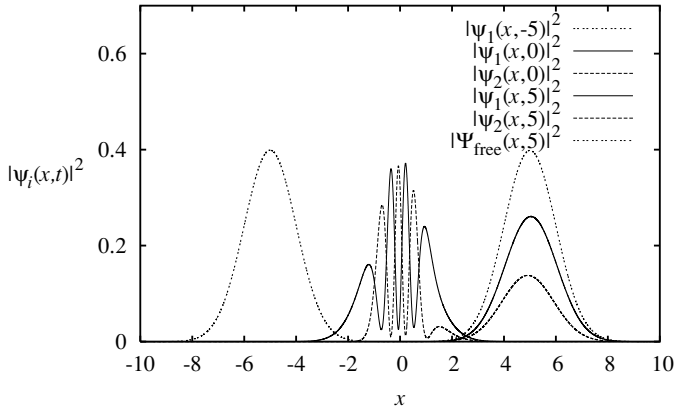

Figure 5. Wave packet propagation for an initial Gaussian wave packet with $v = 1$ and $\Delta = 1$. The parameters of the system are $m = 100$, $\epsilon_1 = 0$, $\epsilon_2 = 1$, $\lambda = 10$ and $\beta = 1$.

particle can be represented, especially if the half-life is large, by a ϕ function of the following form,

$$\phi_b(x - x_0) = \sqrt{\rho(x - x_0)} \tag{10}$$

with

$$\rho(x) = \frac{\Gamma}{v} \exp\left(\frac{\Gamma x}{v}\right) F(x) \tag{11}$$

where $F(x) = \theta(-x) = 0(1)$ if $x > 0$ ($x < 0$). The function $\rho(x - x_0)$ grows exponentially with x. It has a peak at $x = x_0$ where the wave packet is cut off. In order to make the numerical work more tractable we choose a 'smoothed' version of the Heaviside function $\theta(-x)$, i.e., $[1 + \tanh(-\eta x)]/2$, so that $\phi_b(x - x_0)$ grows exponentially with increasing x until $x \approx x_0$,

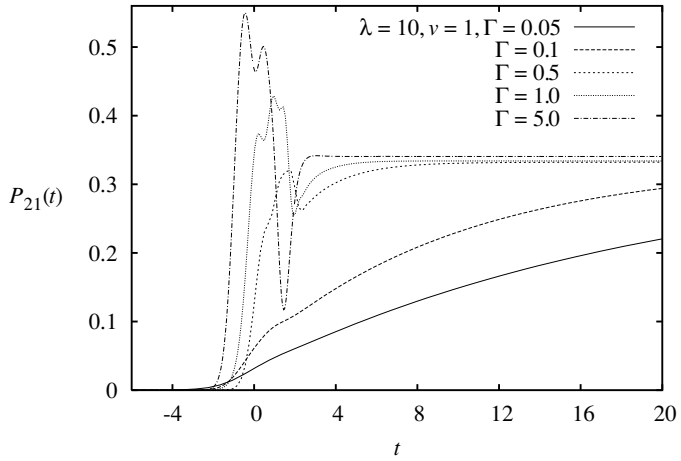

Figure 6. Transition probability from state 1 to state 2 for an exponential wave packet with speed $v = 1$ and different widths. The parameters are $m = 100$, $\epsilon_1 = 0$, $\epsilon_2 = 1$, $\lambda = 10$ and $\beta = 1$.

beyond which it is smoothly, yet steeply, reduced to zero. For a normalized wave packet, $F(x)$ then takes the form

$$F(x) = \frac{\eta v}{\pi \Gamma} \sin\left(\frac{\pi \Gamma}{2\eta v}\right) [1 + \tanh(-\eta x)]. \tag{12}$$

In the numerical work we set $\eta = 15\Gamma/v$. The peak of the function occurs at a value of x that is slightly less than x_0.

We choose x_0 such that $x_0 \ll -1/\beta$ and $x_0 \ll -1/\eta$. The second condition is needed because the smearing causes the front of the wave packet to fall to zero further to the right than in the unsmeared case. The wavefunction $\psi_1(x, t)$, which at $t = t_0$ is $\phi_b(x - x_0)\, \mathrm{e}^{\mathrm{i}k(x-x_0)}$, simulates the wavefunction of an α particle emitted by an α-active nucleus. Apart from the smoothing feature, this form of the wavefunction of a particle emitted from a decaying system has been discussed by Breit [25] and more recently by us [26]. That this shape is a valid representation can be seen by comparing it with the exact wavefunction obtained in [27, 28].

We solve equation (5) with the initial wave packet of the (smoothed) cutoff exponential form. We choose the initial time $t_0 = -10/\beta - 5/\eta$. The peak of an unsmeared wave packet would be at $x = x_0$ at this time. The smearing causes the peak of the initial smeared wave packet to be slightly to the left of x_0.

Figure 6 shows the transition probabilities due to the passage of the cutoff exponential wave packet as a function of time. The interaction with the two-level system begins well before $t = 0$. This is because the front peak of the wave packet is smeared out in time. Table 2 shows the values obtained for $P_{21}(\infty)$ in this case. A comparison with the values tabulated in table 1 shows that the exponential and Gaussian cases yield similar asymptotic transition probabilities.

Figure 7 shows the shapes of the propagating exponential wavefunction at different times, and, at the latest time shown, compares them with a freely propagated exponential wavefunction.

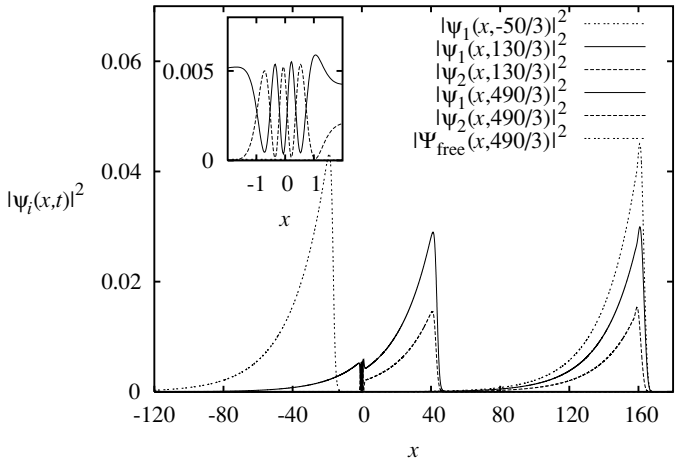

Figure 7. Wave packet propagation for an exponential wave packet with $v = 1$ and $\Gamma = 0.05$. The parameters of the system are $m = 100$, $\epsilon_1 = 0, \epsilon_2 = 1, \lambda = 10$ and $\beta = 1$. Note that $\psi_2(x, t_0) = 0$.

Table 2. Numerical results for $P_{21}(\infty)$ for the exponential wave packet for different values of Γ and λ when $m = 100$, $\epsilon_1 = 0$, $\epsilon_2 = 1$, $v = 1$ and $\beta = 1$.

	$\lambda = 0.1$	$\lambda = 2.0$	$\lambda = 10.0$
$\Gamma = 0.05$	0.006 074	0.437 36	0.330 95
$\Gamma = 0.1$	0.006 074	0.437 36	0.331 00
$\Gamma = 0.5$	0.006 074	0.437 18	0.332 18
$\Gamma = 1.0$	0.006 074	0.436 69	0.334 09
$\Gamma = 5.0$	0.006 044	0.429 68	0.340 62

3. Semi-classical approximations

As an approximation to the quantum system studied in section 2, we now replace the quantum wave packet with a classical particle moving at constant speed. We study two cases: first, a classical point particle and second, a classical particle with finite extension. In each case we compare the numerical result of $P_{21}(t)$ to that obtained by the corresponding fully quantum mechanical calculation using a wave packet. In addition, we study the conditions under which the adiabatic approximation holds. In this approximation, one finds excitations occurring during the scattering process but when the particle has passed through the interaction region the two-level system is found to be again in its initial state.

3.1. Excitations due to the passage of a classical point particle

We assume a classical point particle travelling from left to right. Its position is well defined as $x = vt$ where v is the velocity. The Hamiltonian of this model is

$$H_I = H_0 + V(vt)(|1\rangle\langle 2| + |2\rangle\langle 1|). \tag{13}$$

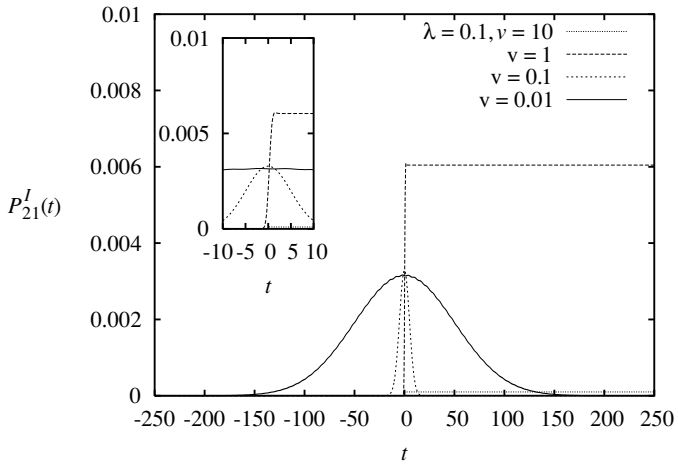

Figure 8. Transition probability from state 1 to state 2 as a function of time for four different velocities using the classical point-particle approximation. The parameters are $\epsilon_1 = 0, \epsilon_2 = 1$, $\lambda = 0.1$ and $\beta = 1$.

The mass of the particle does not appear here. This essentially means that we are assuming an infinitely large mass. We solve the time-dependent Schrödinger equation for the two-level system,

$$\left(\mathrm{i}\frac{\mathrm{d}}{\mathrm{d}t} - H_I\right)\Psi_I(t) = 0 \tag{14}$$

where

$$\Psi_I(t) = a_1(t)|1\rangle + a_2(t)|2\rangle \tag{15}$$

with $a_1(-\infty) = 1$ and $a_2(-\infty) = 0$. Note that t is the only variable in equation (14). The excitation probability at time t is given by

$$P_{21}^I(t) = |a_2(t)|^2. \tag{16}$$

We solve equation (14) numerically for the Gaussian potential function $V(x)$ given in equation (4). Note that for a square-well or δ-function form of the interaction one can obtain analytical solutions as outlined in appendix B.

Figures 8, 9 and 10 show graphs of $P_{21}^I(t)$ versus t for different values of λ and v. In these plots, the shape of a particular curve gives an indication of the adiabaticity of the process. For example, the process is adiabatic for $v = 0.01$ and $v = 0.1$ because the excitation probabilities first rise to non-zero values, but drop asymptotically to zero. For a large speed, i.e. for $v = 10$, the sudden approximation seems appropriate, whereas for $v = 1$ neither the adiabatic nor the sudden approximation is appropriate.

The classical point-particle approximation gives results that are good approximations to those of the fully quantum mechanical analysis in the large-time limit. This remarkable feature is evident from the results listed in table 1. For stronger interactions the agreement decreases, but the approximation still gives the correct order of magnitude for the transition probability.

Table 3 compares the asymptotic transition probabilities $P_{21}(\infty)$ obtained by using quantum mechanical plane waves (i.e. with $\Delta = \infty$) with those obtained by using a classical point particle. (For details of the calculation see appendixn A.) The approximate agreement between the two holds well, provided that the kinetic energy $\frac{1}{2}mv^2$ (which, for example, is

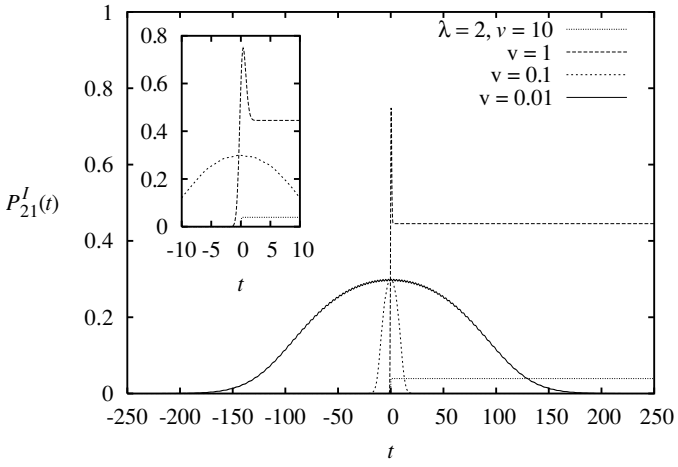

Figure 9. Transition probability as in figure 8 except that $\lambda = 2$.

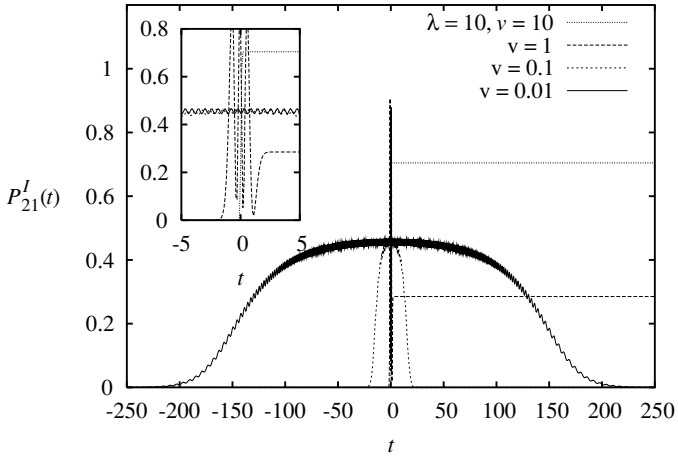

Figure 10. Transition probability as in figure 8 except that $\lambda = 10$.

12.5 when $v = 0.5$) of the incident particle is larger than the excitation energy of the target and the strength of the interaction $\lambda\beta/\sqrt{\pi}$. Let us add that, as v becomes smaller, it becomes more difficult to solve the time-dependent Schrödinger equation (5) numerically, because the time interval over which one has to integrate the equation increases in proportion to $1/v$. For this reason, we do not show the results of the wave packet calculations for $v < 1.0$. (In the case of $\Delta = \infty$, however, the problem can be reduced to that of a stationary state, which is straightforward to handle.) On the other hand, equation (14), in which t is the only variable, can easily be solved for any value of v.

We suspect that the approximate agreement between the classical point particle and the quantum mechanical wave packet results holds when Δ is finite provided v is not too small. This seems to follow from a comparison of the results given in tables 1 and 2. As we point out in appendix B, however, this agreement fails, although only by a factor of 2 or so, when the range $1/\beta$ of $V(x)$ becomes very small.

Table 3. The asymptotic transition probabilities $P_{21}(\infty)$ for the excitations for a classical point particle and for a quantum plane wave for a range of velocities. The parameters are $m = 100$, $\epsilon_1 = 0$, $\epsilon_2 = 1$, and $\beta = 1$.

	$\lambda = 0.1$	$\lambda = 2.0$	$\lambda = 10.0$
Classical point projectile			
$v = 0.15$	0.000 000	0.000 22	0.009 14
$v = 0.20$	0.000 000	0.006 45	0.006 55
$v = 0.50$	0.005 324	0.243 17	0.449 40
$v = 1.00$	0.006 044	0.445 26	0.285 06
Quantum plane wave ($\Delta = \infty$)			
$v = 0.15$	0.000 000	0.001 03	0.006 23
$v = 0.20$	0.000 000	0.002 48	0.063 63
$v = 0.50$	0.005 097	0.246 21	0.332 00
$v = 1.00$	0.006 074	0.437 37	0.330 93

3.2. Excitations due to the passage of an extended classical particle

As a classical approximation to the wave packets of various sizes that we studied earlier, we now consider the classical travelling particle model as in section 3.1 except that we assume that the particle has an extended structure. The centre or the front peak of the particle is at $x(t) = vt$, and the particle has a density distribution $D(x - vt)$. We furthermore assume that the structure of the particle is rigid, i.e., it remains the same in terms of $D(x)$. The Hamiltonian of this model is

$$H_{II} = H_0 + W(t)(|1\rangle\langle 2| + |2\rangle\langle 1|) \tag{17}$$

where $W(t)$ is the interaction obtained by folding $V(x)$ with the density $D(x - vt)$,

$$W(t) = \int_{-\infty}^{\infty} V(x)D(x - vt)\,\mathrm{d}x. \tag{18}$$

For the function $D(x)$ we consider the following two versions, corresponding to the travelling Gaussian wave packet and the cutoff exponential wave packet,

$$D_a(x) = \frac{1}{\sqrt{2\pi}\sigma}\exp\left(-\frac{x^2}{2\sigma^2}\right) \tag{19}$$

$$D_b(x) = \frac{\gamma}{v}\exp\left(\frac{\gamma x}{v}\right)\theta(-x). \tag{20}$$

The function $D_b(x)$ is the same as the probability density distribution of equation (11) except that Γ is here replaced by γ. We do not use the smoothing function of equation (12) here because the effective potential function $W_b(t)$ given below is already a smooth function. To smooth $D_b(x)$ would result in a negligible difference. We obtain the two forms for $W(t)$,

$$W_a(t) = \frac{\lambda}{\sqrt{2\pi}\sigma'}\exp\left(-\frac{v^2t^2}{2\sigma'^2}\right) \qquad \sigma'^2 = \sigma^2 + \frac{1}{2\beta^2} \tag{21}$$

$$W_b(t) = \frac{\lambda\gamma}{2v}\exp\left[-\gamma t + \left(\frac{\gamma}{2\beta v}\right)^2\right]\mathrm{erfc}(-y) \tag{22}$$

where

$$y = \beta vt - \frac{\gamma}{2\beta v}. \tag{23}$$

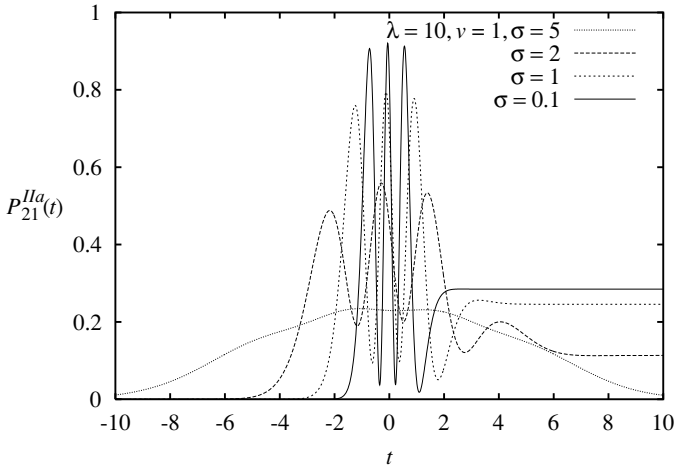

Figure 11. Transition probability as a function of time for the passage of an extended classical particle with a Gaussian distribution. The parameters not shown on the graph are $m = 100$, $\epsilon_1 = 0$, $\epsilon_2 = 1$ and $\beta = 1$.

Table 4. The asymptotic transition probabilities $P_{21}^{IIa}(\infty)$ for the extended classical particle with a Gaussian distribution. The parameters are the same as those of figure 11. Note that as $\sigma \to 0$, the results for the extended classical particle reduce to those of the classical point particle.

	$\lambda = 0.1$	$\lambda = 2.0$	$\lambda = 10.0$
$\sigma = 0.001$	0.006 044	0.445 26	0.285 03
$\sigma = 0.01$	0.006 043	0.445 20	0.285 05
$\sigma = 0.1$	0.005 984	0.439 70	0.284 76
$\sigma = 1$	0.002 223	0.120 78	0.245 59
$\sigma = 2$	0.000 110	0.000 39	0.113 23
$\sigma = 5$	0.000 000	0.000 00	0.000 02
Classical point	0.006 044	0.445 26	0.285 06

For large $|y|$ the argument of the exponential function becomes too large for a numerical evaluation of $W_b(t)$. We then use the asymptotic expansion [29],

$$W_b(t) \sim -\frac{\lambda\gamma\, \mathrm{e}^{-\beta^2 v^2 t^2}}{2\sqrt{\pi}vy}\left[1 + \sum_{j=1}^{\infty}(-1)^j \frac{1\cdot 3\cdots(2j-1)}{(2y^2)^j}\right]. \tag{24}$$

We denote the transition probabilities as $P_{21}^{IIa}(t)$ and $P_{21}^{IIb}(t)$, respectively.

In figure 11 we compare $P_{21}^{IIa}(t)$ for different sizes of the classical particle. For $P_{21}^{IIa}(\infty)$ there is clearly a dependence on the size, which was absent in the wave packet calculations. As the size increases, $P_{21}^{IIa}(\infty)$ decreases. See also table 4. When the extension of the particle is substantially larger than the interaction region the process appears to behave adiabatically and $P_{21}^{IIa}(\infty)$ is negligible.

Figure 12 shows the behaviour of the transition probability as a function of time for the extended classical particle when its distribution is taken to be a truncated exponential. As was the case for the classical Gaussian distribution, the onset of the adiabaticity in this case also causes $P_{21}^{IIb}(t)$ to decrease as the spatial extent of the travelling object increases. In table 5

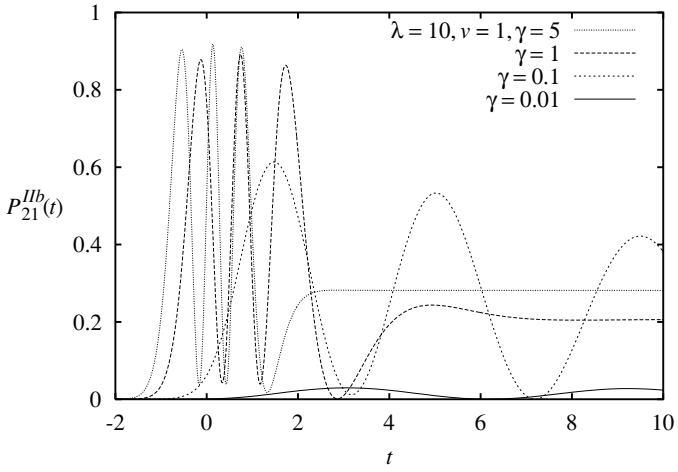

Figure 12. Transition probability as a function of time for the passage of an extended classical particle with a truncated exponential distribution. The parameters not shown on the graph are $m = 100$, $\epsilon_1 = 0$, $\epsilon_2 = 1$ and $\beta = 1$.

Table 5. The asymptotic transition probabilities $P_{21}^{IIb}(\infty)$ for the extended classical particle with exponential distribution. The parameters are the same as those of figure 12. As $\gamma \to \infty$ the results reduce to those of the classical point particle.

	$\lambda = 0.1$	$\lambda = 2.0$	$\lambda = 10.0$
$\gamma = 0.01$	0.000 001	0.000 242	0.005 862
$\gamma = 0.1$	0.000 060	0.021 269	0.135 696
$\gamma = 1.0$	0.003 022	0.255 043	0.206 044
$\gamma = 2.0$	0.004 835	0.354 134	0.246 413
$\gamma = 5.0$	0.005 812	0.424 841	0.281 589
$\gamma = 10.0$	0.005 984	0.439 799	0.284 592
$\gamma = 50.0$	0.006 042	0.445 035	0.285 044
$\gamma = 100.0$	0.006 043	0.445 202	0.285 053
$\gamma = 200.0$	0.006 044	0.445 244	0.285 055

we show the values of $P_{21}^{IIb}(\infty)$, further demonstrating that the adiabatic limit plays a role in reducing $P_{21}^{IIb}(\infty)$ as the structure of the particle becomes more extended.

4. Summary and discussion

In this paper, we have questioned the validity of a classical treatment of an α particle that interacts with and (possibly) excites an atom. In order to gain insight into this question we have examined a model which simulates the interaction of an α particle and an atom. A particle in one dimension impinges on and excites a two-level system. We assume in most cases of the calculations that the kinetic energy of the incident particle is much larger than the excitation energy of the target. We treat the particle in two ways: as a quantum mechanical wave packet, and as a classical particle.

We have found several interesting features regarding the excitation probability $P_{21}(t)$ for the two-level system. These are summarized in the following:

(i) In the quantum treatment of the incident particle with an energy much larger than the excitation energy, the asymptotic transition probability $P_{21}(\infty)$ is remarkably insensitive to the size and shape of the wave packet. A wave packet and a plane wave lead to almost the same values for $P_{21}(\infty)$, even for quite narrow wave packets. We examined the case such that the width of the wave packet is as small as $\Delta = 0.1$, which is $1/10$ of the Bohr radius, much smaller than the atomic size.

It is well known that the usage of the plane wave, which is not normalizable, can be justified by starting with a broad wave packet and letting the width tend to infinity [30]. The degree of the insensitivity to the size of wave packet over such a wide range that we have found is a new result as far as we know. The process under consideration is intrinsically a time-dependent one. In the plane wave limit, however, the problem is reduced to that of a stationary state.

(ii) The transition probabilities have quite a complicated time dependence during the finite time interval in which the wave packet or the classical point particle is interacting with the two-level system. The details of the transition probability curves are sensitive to the size and shape of the wave packet and to whether the particle is a quantum mechanical or a classical point particle. This feature makes it all the more remarkable that such varied forms of $P_{21}(t)$ all converge to nearly the same asymptotic value $P_{21}(\infty)$.

(iii) The lack of sensitivity of the asymptotic quantum transition probabilities to the starting position of the incident wave packet is another remarkable feature. One might expect that wave packets started at a greater distance from the interaction region would behave like broader wave packets started closer and hence the same variation, although small, of wave packets of different widths would occur for wave packets of the same width with different starting positions. In fact, the asymptotic transition probabilities of wave packets with the same initial widths but different starting positions are exactly equal, although the transition probabilities for finite times are very different.

(iv) In the classical treatment of the particle, in contrast, we find that $P_{21}(\infty)$ is sensitive to the size of the particle. The values obtained for $P_{21}(\infty)$ for a point particle are close to those obtained for the quantum mechanical wave packet (of any size and shape). This implies, as far as our model and $P_{21}(\infty)$ are concerned, that the particle can approximately be treated as a classical point particle.

(v) As the size of the classical particle becomes very large, the interaction $V(vt)$ between the particle and the two-level system becomes a very slowly varying function of t, and consequently $P_{21}(\infty)$ becomes very small. (The same would happen for a point particle ($\sigma = 0$), but a long-range interaction (β small) as is evident from equation (21). However, such a long-range interaction is beyond the scope of the discussion of this paper.) This behaviour is consistent with the adiabatic theorem.

In the features summarized above, it is understood that in the quantum case the speed v of the incident particle is so large that the kinetic energy of the particle is much larger than the excitation energy of the two-level system. Such a speed is appropriate in the simulation of an α particle that impinges on an atom. We have also examined cases with smaller values of v but for a classical point particle and for a quantum mechanical wave packet with an infinite width, i.e., a plane wave. The approximate agreement between the quantum mechanical and classical calculations continues to hold for smaller values of v. If the range of the interaction becomes very small and consequently the local strength of the interaction very large, the agreement deteriorates. We assumed $m = 100$ for the mass of the particle. This is not as large as the mass of the α particle, which is about 8×10^3. The features that we have summarized above, however, remain valid when we increase the value of m. For smaller values of m, we suspect

that the situation remains similar provided that $\frac{1}{2}mv^2$ is much larger than the excitation energy $\epsilon_2 - \epsilon_1$ and the interaction strength.

Note that there is an important difference between a classical particle travelling with a specified speed through an atom or a detector and exciting it, and a quantum mechanical particle or a wave packet that has been ejected from a decaying system and also excites an atom or a detector. In the latter case the speed of the particle, if we interpret it as the rate of the change in time in the expectation value of the position as a function of time, tends to be far smaller as compared with the speed that is assumed for the corresponding classical particles. (The speed in fact increases and approaches the constant speed of the classical counterpart, but only towards the end of the decay process.) The difference becomes especially significant if the half-life of the decaying system is large [7, 9].

As we mentioned in section 1, the problem of the atomic ionization caused by the nuclear α decay was re-examined recently [7–9]. It was found that a fully quantum mechanical, time-dependent calculation in a model simulation gives an ionization probability that is orders of magnitude smaller than those of the traditional calculation with a classical α particle. Feature (iv) summarized above, however, seems to be inconsistent with the results of [7–9]. Furthermore, feature (i) seems to rationalize the stationary or quasi-stationary approach taken by Révai and Nogami in their attempt at justifying the classical treatment of the α particle [6]. A critical scrutiny of the model calculation of [7–9] is the subject of our next project.

Acknowledgments

We would like to thank Eve Stencel for her help in the calculation of the plane wave case. This work was supported by the Natural Sciences and Engineering Research Council of Canada (NSERC). KAK was supported by an award from Research Corporation and AP was supported by the Science Research Training Program at Taylor University. KS acknowledges the NSERC Undergraduate Summer Research Awards received during the summers of 1999–2001.

Appendix A. Case with an incident plane wave

For the case of an incident plane wave the problem can be reduced to that of a stationary state. The wavefunction $\Psi(x, t)$ of equation (6) can be written as $\Psi(x, t) = \Phi(x)\mathrm{e}^{-\mathrm{i}Et}$ where E is the energy of the entire system and

$$\Phi(x) = \begin{cases} (\mathrm{e}^{\mathrm{i}k_1 x} + R_{11}\mathrm{e}^{-\mathrm{i}k_1 x})|1\rangle + R_{21}\mathrm{e}^{-\mathrm{i}k_2 x}|2\rangle & x \ll 0 \\ T_{11}\mathrm{e}^{\mathrm{i}k_1 x}|1\rangle + T_{21}\mathrm{e}^{\mathrm{i}k_2 x}|2\rangle & x \gg 0. \end{cases} \tag{A.1}$$

The momenta k_1 and k_2 are both positive and are related to the energy E by

$$E = \epsilon_1 + \frac{k_1^2}{2m} = \epsilon_2 + \frac{k_2^2}{2m}. \tag{A.2}$$

Note that k_1 has been denoted by k in the main body of this paper. The transmission and reflection amplitudes are denoted by T_{ij} and R_{ij}, respectively, so that T_{21}, for example, denotes the transmission amplitude for a transition of the two-level system from state 1 to state 2.

Probability current continuity leads to

$$|T_{11}|^2 + |R_{11}|^2 + \frac{k_2}{k_1}(|T_{21}|^2 + |R_{21}|^2) = 1. \tag{A.3}$$

We use P_{ji} to denote the probability that the two-level system is initially in state i and finally in j. We obtain

$$P_{11} = |T_{11}|^2 + |R_{11}|^2 \qquad P_{21} = 1 - P_{11}. \tag{A.4}$$

These are both independent of time.

As a special example let us assume the potential

$$V(x) = \lambda\delta(x). \tag{A.5}$$

This is the $\beta \to \infty$ limit of $V(x)$ of equation (4). In this case the Schrödinger equation can be solved easily and we obtain

$$T_{11} = \frac{k_1k_2}{\lambda^2m^2 + k_1k_2} \qquad R_{11} = \frac{-\lambda^2m^2}{k_1k_2 + \lambda^2m^2} \qquad R_{21} = T_{21} = \frac{-\mathrm{i}\lambda mk_1}{\lambda^2m^2 + k_1k_2}. \tag{A.6}$$

Note that $R_{21} = T_{21}$. This means that the memory of the direction of the incident particle in channel 1 has been lost completely in channel 2. This does not occur if $V(x)$ is smeared out. The transition probability is given by

$$P_{21} = \frac{2\lambda^2m^2k_1k_2}{(\lambda^2m^2 + k_1k_2)^2}. \tag{A.7}$$

If the speed v of the incident particle is so large that $v \gg \lambda$ and $\frac{1}{2}mv^2 \gg (\epsilon_2 - \epsilon_1)$, then P_{21} is reduced to

$$P_{21} \to \frac{2\lambda^2m^2}{k_1k_2} \to 2\left(\frac{\lambda}{v}\right)^2. \tag{A.8}$$

In section 3.1 we numerically obtain P_{21} when the interaction is that of equation (4). This can, in principle, be done by integrating the time-independent Schrödinger equation from $x = \infty$ to $x = -\infty$ twice, first with initial conditions ($\psi_1(x) = \mathrm{e}^{-\mathrm{i}k_1x}$, $\psi_2(x) = 0$) and then again with initial condition ($\psi_1(x) = 0, \psi_2(x) = \mathrm{e}^{-\mathrm{i}k_2x}$). The two solutions at $x = -\infty$ can be combined to obtain the transition amplitudes. This method breaks down when the potential is strongly repulsive since then the two sets of initial conditions tend to converge to the same solution. An approach that avoids having to find two solutions and involves integrating coupled first-order differential equations is the variable-phase method [31, 32]. We use this method when the other one fails.

Appendix B. Analytic solutions for the point-particle case

We can write equation (14) in matrix form

$$\mathrm{i}\frac{\mathrm{d}\mathbf{a}(t)}{\mathrm{d}t} = M(t)\mathbf{a}(t) \tag{B.1}$$

$$\mathbf{a}(t) = \begin{pmatrix} a_1(t) \\ a_2(t) \end{pmatrix} \qquad M(t) = \begin{pmatrix} \epsilon_1 & V(vt) \\ V(vt) & \epsilon_2 \end{pmatrix}. \tag{B.2}$$

Equations (B.2) can be solved numerically for a given function $V(x)$. In certain cases we can obtain analytic solutions. Assume a square-well form for $V(x)$, i.e.,

$$V(x) = \begin{cases} V_0 & \text{for} \quad 0 \leqslant x \leqslant b \\ 0 & \text{otherwise.} \end{cases} \tag{B.3}$$

The passing particle experiences a constant interaction over the time interval b/v. The initial conditions are $a_1(0) = 1$ and $a_2(0) = 0$, where t corresponds to the $t - t_0$ of the main body of this paper. We obtain the solution

$$\mathbf{a}(t) = \begin{cases} \mathrm{e}^{-\mathrm{i}M_0t}\mathbf{a}(0) & \text{for} \quad 0 \leqslant t \leqslant b/v \\ \mathrm{e}^{-\mathrm{i}M_0b/v}\mathbf{a}(0) & \text{for} \quad t \geqslant b/v \end{cases} \tag{B.4}$$

$$M_0 = M(0) = \tfrac{1}{2}(\epsilon_1 + \epsilon_2) + \tfrac{1}{2}(\epsilon_1 - \epsilon_2)\sigma_3 + V_0\sigma_1. \tag{B.5}$$

Here and in the next equation σ_1, σ_2 and σ_3 are the standard 2×2 Pauli matrices. The matrix M_0 can be diagonalized by a unitary transformation $M_0 \to U M_0 U^\dagger$ with

$$U = \mathrm{e}^{\mathrm{i}\theta\sigma_2} \qquad \theta = V_0/(\epsilon_1 - \epsilon_2). \tag{B.6}$$

This allows us to write the $\mathbf{a}(t)$ of equation (B.4) explicitly and obtain

$$P_{21}^I(t) = \left(\frac{V_0}{\omega}\right)^2 \sin^2 \omega t \qquad \omega^2 = V_0^2 + \frac{1}{4}(\epsilon_1 - \epsilon_2)^2 \tag{B.7}$$

for $0 \leqslant t \leqslant b/v$. This result was also obtained in problem (179) of [33]. The transition probability $P_{21}^I(t)$ for $t \geqslant b/v$ can be obtained from equation (B.7) with $t = b/v$. The transition probability $P_{21}^I(t)$ fluctuates during the time period in which the interaction takes place. This aspect is similar to the fluctuations of $P_{21}^I(t)$ seen in figures 11 and 12.

A special case of the interaction potential is obtained by letting $V_0 \to \infty$ and $b \to 0$ but keeping the product $V_0 b = \lambda$ fixed. Then we obtain the δ-function interaction potential $V(x) = \lambda\delta(x)$. The transition probability of this case is

$$P_{21}^I(t) = \sin^2(\lambda/v) \qquad t > 0. \tag{B.8}$$

If $\lambda/v \ll 1$ we obtain $P_{21}^I(\infty) = (\lambda/v)^2$, which is a half of the P_{21}^I of equation (A.8). This difference is related to the fact that $R_{21} = T_{21}$ in the plane wave case; i.e. in channel 2 the wave proceeds equally in the forward and backward directions. In contrast, the classical particle moves always forwards at constant speed v.

References

[1] Migdal A 1941 *J. Phys. (USSR)* **4** 449
[2] Levinger J S 1953 *Phys. Rev.* **90** 11
[3] Fishbeck H J and Freedman M S 1975 *Phys. Rev. Lett.* **34** 172
[4] Fishbeck H J and Freedman M S 1977 *Phys. Rev.* A **15** 162
[5] Mott N F 1929 *Proc. R. Soc.* A **126** 79
[6] Rèvai J and Nogami Y 1992 *Few-Body Syst.* **13** 75
[7] Kataoka F 1998 Atomic ionization following α-decay of the nucleus *Master's Thesis* McMaster University (unpublished)
[8] Kataoka F, Nogami Y and van Dijk W 2000 *J. Phys. A: Math. Gen.* **33** 5547
[9] Nogami Y and van Dijk W 2001 *Few-Body Syst. Suppl.* **13** 196
[10] D'Arrigo A, Eremin N V, Fazio G, Giardina G, Glotova M G, Klochko T V, Sacchi M and Taconne A 1994 *Phys. Lett.* B **332** 25
[11] Kasagi J, Yamazaki H, Ohtsuki Y and Yuki H 1997 *Phys. Rev. Lett.* **79** 371
[12] Papenbrock T and Bertsch G F 1998 *Phys. Rev. Lett.* **80** 4141
[13] Flambaum V V and Zelevinsky V G 1999 *Phys. Rev. Lett.* **83** 3108
[14] Takigawa N, Nozawa Y, Hagino K, Ono A and Brink D M 1999 *Phys. Rev.* C **59** R593
[15] Bertulani C A, de Paula D T and Zelevinsky V G 1999 *Phys. Rev.* C **60** 0316021
[16] Unruh W G and Wald R M 1984 *Phys. Rev.* D **29** 1047
[17] Blanchard P and Jadczyk A 1996 *Helv. Phys. Acta* **69** 613
[18] Kiers K and Weiss N 1998 *Phys. Rev.* D **57** 3091
[19] Herrick D R and Stillinger F H 1975 *Phys. Rev.* A **11** 42
[20] Lapidus I R 1975 *Am. J. Phys.* **43** 790
[21] Nogami Y, Vallières M and van Dijk W 1976 *Am. J. Phys.* **44** 886
[22] Mişicu S, Rizea M and Greiner W 2001 *J. Phys. G: Nucl. Part. Phys.* **27** 993
[23] Tal-Ezer H and Kosloff R 1984 *J. Chem. Phys.* **81** 3967
[24] Leforestier C *et al* 1991 *J. Comp. Phys.* **94** 59
[25] Breit G 1959 *Encyclopedia of Physics* vol 41 (Berlin: Springer) pp 1–407
[26] van Dijk W, Kataoka F and Nogami Y 1999 *J. Phys. A: Math. Gen.* **32** 6347
[27] van Dijk W and Nogami Y 1999 *Phys. Rev. Lett.* **83** 2867

[28] van Dijk W and Nogami Y 2002 *Phys. Rev.* C **65** 024608
[29] Abramowitz M and Stegun I A 1965 *Handbook of Mathematical Functions* (New York: Dover) p 298
[30] Goldberger M A and Watson K M 1964 *Collision Theory* (New York: Wiley)
[31] van Dijk W and Razavy M 1979 *Can. J. Phys.* **57** 1952
[32] van Dijk W and Razavy M 1979 *Int. J. Quantum Chem.* **16** 1249
[33] Flügge S 1974 *Practical Quantum Mechanics* (New York: Springer)